1,4-Disilacyclohexa-2,5-diene: A Molecular Building Block that Allows for Remarkably Strong Neutral Cyclic Cross-Hyperconjugation

Julius Tibbelin,[a] Andreas Wallner,[a,f] Filip Heijkenskjöld,[b] Rikard Emanuelsson,[a] Martin Rosenberg,[a,c] Kaoru Yamazaki,[a,d] Djawed Nauroozi,[e] Leif Karlsson,[b] Raimund Feifel,[b]* Roland Pettersson,[a] Judith Baumgartner,[f] Sascha Ott,[e] and Henrik Ottosson [a]*

[a] Department of Chemistry – BMC, Box 576, Uppsala University, 751 23 Uppsala, Sweden, [b] Department of Physics and Astronomy, Box 516, Uppsala University, 751 20 Uppsala, Sweden, [c] Department of Chemistry, University of Copenhagen, Universitetsparken 5, 2100 Copenhagen Ø, Denmark, [d] Department of Chemistry, Graduate School of Science, Tohoku University, Sendai 980-8578, Japan, [e] Department of Chemistry – Ångström laboratory, Uppsala University, Box 523, 751 20 Uppsala, Sweden, [f] Institut für Anorganische Chemie, Technische Universität Graz, Stremayrgasse 9, A-8010 Graz, Austria.

* E-mail: Henrik.Ottosson@kemi.uu.se

Raimund.Feifel@physics.uu.se

Table-of-contents

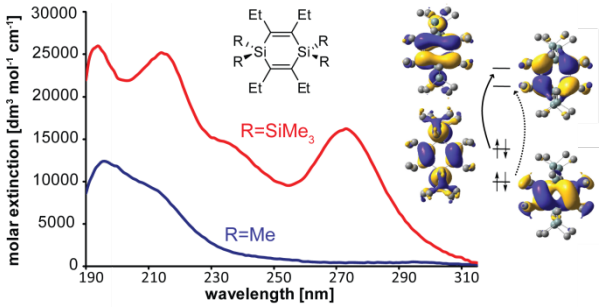

The fusion of two cross-hyperconjugated segments in form of the small 1,4-disilacyclohexa-2,5-diene cycle provides for electronic and optical properties which resemble to those of π-conjugated cycles.

Abstract: The electronic structures of 2,3,5,6-tetraethyl-1,4-disilacyclohexa-2,5-dienes with either four chloro (**1a**), methyl (**1b**), or trimethylsilyl (TMS) (**1c**) substituents at the two silicon atoms were examined in an effort to design cyclic compounds with strong neutral cross-hyperconjugation between π- and σ-bonded segments. Remarkable variations in the lowest electronic excitation energies, lowest ionization energies, and the first oxidation potentials were observed upon change of substituents, as determined by gas phase ultraviolet (UV) absorption spectroscopy, ultraviolet photoelectron spectroscopy (UPS), and cyclic voltammetry. The spectroscopic studies reveal a particularly strong neutral cyclic cross-hyperconjugation in **1c**. Its lowest electron binding energy (7.1 eV) is distinctly different from that of **1b** (8.5 eV) and cyclohexa-1,4-diene (8.8 eV). Molecular orbital analysis reveals a significantly stronger interaction between filled π(C=C) and π(SiR_2) group orbitals in **1c** than in **1a** and **1b**. The energy shift in the highest occupied molecular orbital is also reflected in the first oxidation potentials as observed in the cyclic voltammograms of the respective compounds (1.47, 0.88, and 0.46 V for **1a**, **1b** and **1c**, respectively). Furthermore, 1,4-disilacyclohexadiene **1c** absorbs strongly at 273 nm (4.55 eV), whereas **1a** and **1b** have no symmetry allowed excitations above 215 nm (below 5.77 eV). The fusion of two trisilane and two olefin fragments in form of the cyclic compound **1c** clearly leads to a new chromophore with markedly different spectroscopic features than the separated fragments. Suitably substituted 1,4-disilacyclohexa-2,5-dienes represent novel building blocks for the design of larger cross-hyperconjugated molecules as alternatives to traditional purely cross-π-conjugated analogues.

Introduction

π-Conjugation and σ-conjugation are well-established concepts in chemistry since many decades, and an enormous number of compounds which exhibit either of these conjugation topologies have been investigated for purely fundamental reasons as well as in the course of development in a range of different applied areas.[1-3] However, the combination of the two conjugation topologies into a strong σ/π-conjugation, or hyperconjugation, in a neutral compound is less explored,[4] and even much less exploited in applications. Herein, we report on a joint theoretical and experimental study of a compound class, the 1,4-disilacyclohexa-2,5-dienes (**1**, Figure 1), in which π- and σ- bonded molecular segments interact in a cyclic cross-hyperconjugated manner and for which the interaction strength can be varied extensively by the choice of substituents.[5] These species could potentially rival 1-silacyclopenta-2,4-dienes (siloles), organosilicon compounds which are extensively investigated and which have similar electronic properties to thiophenes. Due to this similarity the silole molecule and its oligomers and polymers (Figure 2) find applications in organic electronics.[6]

σ-Conjugation is observed in heavy alkanes, such as oligo- and polysilanes.[2] A strong mix of σ- and π-conjugation is therefore exceptionally rare in neutral pure hydrocarbons even though such neutral hyperconjugation is observed in the recent perfluoroaryltetrahedranes (**2**), of Sekiguchi and co-workers, composed of one or two strained tetrahedranes which interact with an adjacent phenyl group.[7] Recently, we examined the electronic structure of *bis*(phenylethynyl)methanes and silanes in dependence of the substituents at the central C or Si atom, and we found that when the substituents at the central atom are σ-electron donor groups such as the trimethylsilyl group the electronic structures of these compounds resemble that of a regular cross-π-conjugated hydrocarbon.[8] Such molecules have two hyperconjugated paths which are united by the π-symmetric group orbital of the central ER_2 moiety having the

same function as a geminally connected C=C double bond. These compounds can therefore be labelled as cross-hyperconjugated. Indeed, hyperconjugative interaction between ethylene fragments bonded to the silicon atom in dimethyldivinylsilane has been shown earlier with photoelectron spectroscopy,[9] but a $SiMe_2$ segment only provides for very weak interaction.8 Similarly, cyclohexa-1,4-diene has been studied theoretically as well as experimentally, both in the ground and the excited states, and weak hyperconjugation has been demonstrated and attributed to $\pi(CH_2)$ group orbitals composed of the C-H σ- and σ*-bond orbitals interacting with the π-orbitals of the C=C double bond.[10]

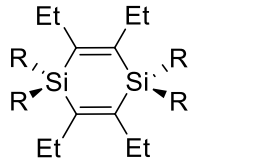

1a R = Cl
1b R = Me
1c R = $SiMe_3$ (TMS)

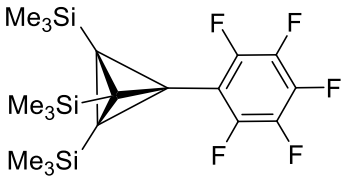

2

Figure 1. The 1,4-disilacyclohexa-2,5-dienes (**1**) examined herein, and an example of the previously investigated neutral hydrocarbon **2** of Sekiguchi and co-workers which display significant neutral hyperconjugative interaction (ref. **7**).

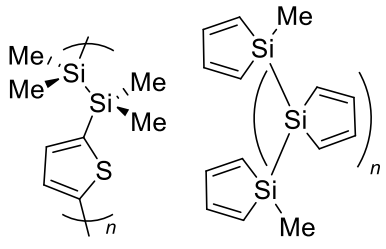

3 **4**

Figure 2. Earlier investigated oligomers and polymers with interacting σ- and π-bonded segments; the silanylene-thiophene (**3**) and silole (**4**) oligomers with six electrons in π(C=C) and π(SiR_2) orbitals (refs. 11-19 and **6**).

Oligomeric and polymeric compound classes which contain σ- and π-bonded segments, *e.g.* the linearly linked silanylene-thiophene oligomers **3** (Figure 2), have been investigated earlier.[11-19] However, the rotational flexibility about the single bonds of the polymer backbone affects the σ/π-coupling strength.[9,10] Poly-1,1-siloles in which the monomers are connected *via* the Si atoms (**5**) reveal significant coupling between the localized π*-orbitals of the diene segment and the delocalized σ*-orbitals (*cf.*, π($Si(SiR_3)_2$ group orbitals) of the Si backbone, respectively.[20] Linear and cyclic oligo-1,1-siloles have also been reported, and the UV absorption spectra of the tetra-, penta-, and hexamers have λ_{max} in the range of 275 - 320 nm.[21-24]

The silole ring has six electrons in orbitals of π-character; four in the π-orbitals of the 1,3-butadiene segment and two in the π(SiR_2) group orbital. Yet, despite the 6π-electron systems, the geometries of various siloles indicate that cyclic conjugation is modest.[25,26] In this context it is noteworthy that the electronic structure of siloles is valence isolobal to that of pentafulvenes (Figure 3), cross-π-conjugated hydrocarbons in which the optical properties and degree of aromaticity can be varied extensively through substitution, from the nonaromatic parent pentafulvene to the aromatic compound when the exocyclic substituent are amino groups.[27-30]

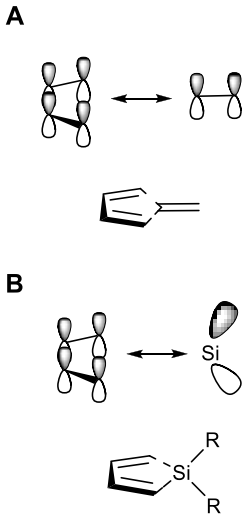

Figure 3. Schematic drawings of the valence isolobal analogy of the interactions between the π-symmetric basis orbitals of (A) pentafulvene and (B) silole, respectively.

Our hypothesis is now that **1** is a useful template for the design of neutral cyclic cross-hyperconjugated molecules. In a similar way that the π-orbital interaction in siloles is valence isolobal with that of pentafulvenes, the π-orbital interaction in **1** is isolobal to that between the π-orbitals of the endocyclic and the exocyclic C=C bonds in *para*-quinodimethane (**5**, Figure 4). *Para*-quinodimethane is a cyclic cross-π-conjugated compound,[10] and by analogy, properly substituted derivatives of **1** are potentially cyclic cross-hyperconjugated. The question thus arises whether 1,4-disilacyclohexa-2,5-diene can provide a template for the design of optically and electronically useful compounds in a similar manner as **5** represents a template for tetracyanoquinodimethane (TCNQ), one of the cornerstones of organic electronics?[31]

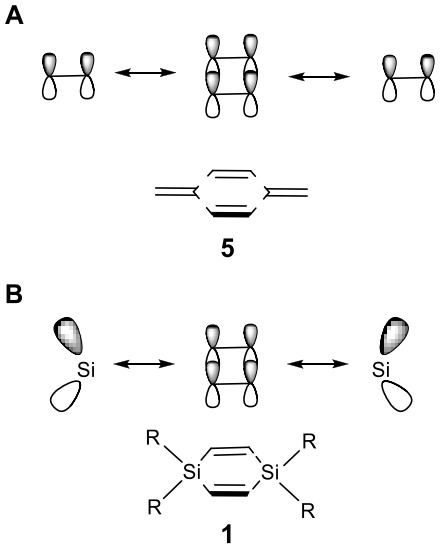

Figure 4. Schematic drawings of the valence isolobal analogy of the interactions between the π-symmetric basis orbitals of (A) *para*-quinodimethane (**5**) and (B) 1,4-disilacyclohexa-2,5-diene (**1**), respectively.

The parent 1,4-disilacyclohexa-2,5-diene (**1**), has a $\Delta\varepsilon_{H\text{-}L}$ of 6.43 eV at B3LYP/6-31G(d,p) level.[32] Although the few earlier experimental studies focused on synthesis rather than spectroscopy,[33-35] it is interesting that the ^{1}H NMR chemical shift of the vinylic protons in 1,1,4,4-tetramethyl-1,4-disilacyclohexa-2,5-diene was found at 6.84 ppm, exceptionally low-field for vinylic protons.[36] In the present study, 1,4-disilacyclohexa-2,5-dienes with either Cl (**1a**), Me (**1b**), or $SiMe_3$ (**1c**, TMS) substituents at the Si atoms and ethyl substituents at the sp^2 hybridized C atoms (Figure 1) were synthesized and examined by X-ray crystallography, gas phase UV absorption spectroscopy, UV photoelectron spectroscopy (UPS), and cyclic voltammetry. As a reference for a non-cross-hyperconjugated compound, the all-carbon analogue, *i.e.*, cyclohexa-1,4-diene (**6**), was also examined by gas phase UV absorption spectroscopy. By quantum chemical calculations the investigation was extended to a larger set of 1,4-disilacyclohex-2-enes and related compounds (Figure 5) so as to reveal the effect of the neutral cyclic cross-hyperconjugation as compared to ordinary neutral linear hyperconjugation

and acyclic cross-hyperconjugation. Properties, such as electronic transitions, ionization potentials, and how these are coupled to the substitution pattern of the different compounds, are analyzed and discussed. Our aim is to deduce a new monomer unit which in an optimal manner combines σ- and π-bonded segments into a rigid and strongly cross-hyperconjugated cyclic framework. This unit could represent a novel structural motif to be used in oligomers and polymers for various optical and/or electronic applications, similar to the silole unit.

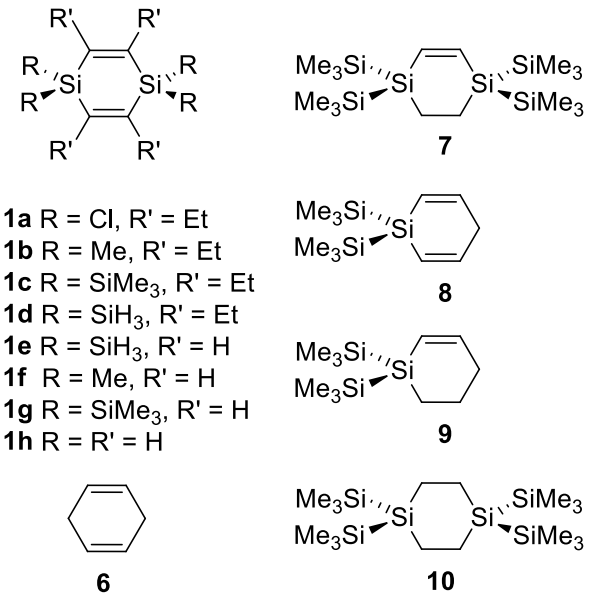

Figure 5. The substituted 1,4-disilacyclohexa-2,5-dienes (**1a** – **1h**), the all-carbon reference cyclohexa-1,4-diene (**6**), and model compounds (**7** - **10**) explored computationally to examine the extent of cyclic cross-hyperconjugation.

Results and Discussion

The goal of the presently reported investigation is to find ways to maximize the neutral cyclic cross-hyperconjugative interaction between the local π(C=C) and π(ER_2) orbitals in 1,4-disilacyclohexa-2,5-dienes **1a** – **1c**. For that reason we first discuss the qualitative molecular orbital (MO) diagram and the calculated MOs before progressing to the experimental data. At the end we compare, through quantum chemical calculations, the strongly cross-

hyperconjugated **1c** with several model compounds (**7** - **10**) which allows for an evaluation of the cyclic cross-hyperconjugation in **1c** as compared to hyperconjugation and acyclic cross-hyperconjugation. One purpose of the study is to show how qualitative MO theory and subsequent quantum chemical calculations can be used as design tools *a priori* to experimental studies, in contrast to the regular *a posteriori* usage of quantum chemical computations (and theory).

Molecular orbitals: Figure 6 shows the MOs of π-symmetry and considers a D_{2h} symmetric 1,4-disilacyclohexa-2,5-diene with substituents R and R' at the silicon and carbon atoms, respectively. These MOs are derived through combinations of suitable local π-orbitals of the two C=C bonds combined into a 2x(C=C) fragment (marked blue in Figure 6) and the two SiR_2 moieties of a 2x(SiR_2) fragment (marked red). The interaction includes the symmetry-adapted in-phase and out-of-phase combinations of the four π_{CC} and π^*_{CC} orbitals of 2x(C=C) with the symmetry-adapted in-phase and out-of-phase combinations of the four π(SiR_2) and π*(SiR_2) orbitals of the 2x(SiR_2) fragment.

The occupied group orbital of b_{1u} symmetry on the 2x(C=C) fragment and the two occupied and unoccupied group orbitals of this symmetry on 2x(SiR_2) combine into the three $1b_{1u}$, $2b_{1u}$, and $3b_{1u}$ MOs of which the first two are occupied. Similarly, the vacant b_{2g} group orbital of 2x(C=C) combine with the two b_{2g} orbitals of the 2x(SiR_2) fragment into the $1b_{2g}$, $2b_{2g}$, and $3b_{2g}$ MOs, where the first one is occupied. One b_{1u} and one a_u orbital also exist on the 2x(C=C) fragment, but neither of these can interact with a suitable π-symmetric orbital at 2x(SiR_2) constructed from two π(SiR_2) or two π*(SiR_2) orbitals. They may instead each interact with the two empty 3d(Si) AOs combined into b_{3g} and a_u symmetric 2x(SiR_2) group orbitals. The interaction between the occupied b_{3g} group orbital of the 2x(C=C) fragment and the vacant b_{3g} orbital of 2x(SiR_2) should be negligible so that the $1b_{3g}$ MO remains localized to the two C=C double bonds. However, the interaction between the vacant a_u group orbital of

2x(C=C) and the vacant a_u orbital of 2x(SiR_2) can, on the other hand, be substantial (*vide infra*).

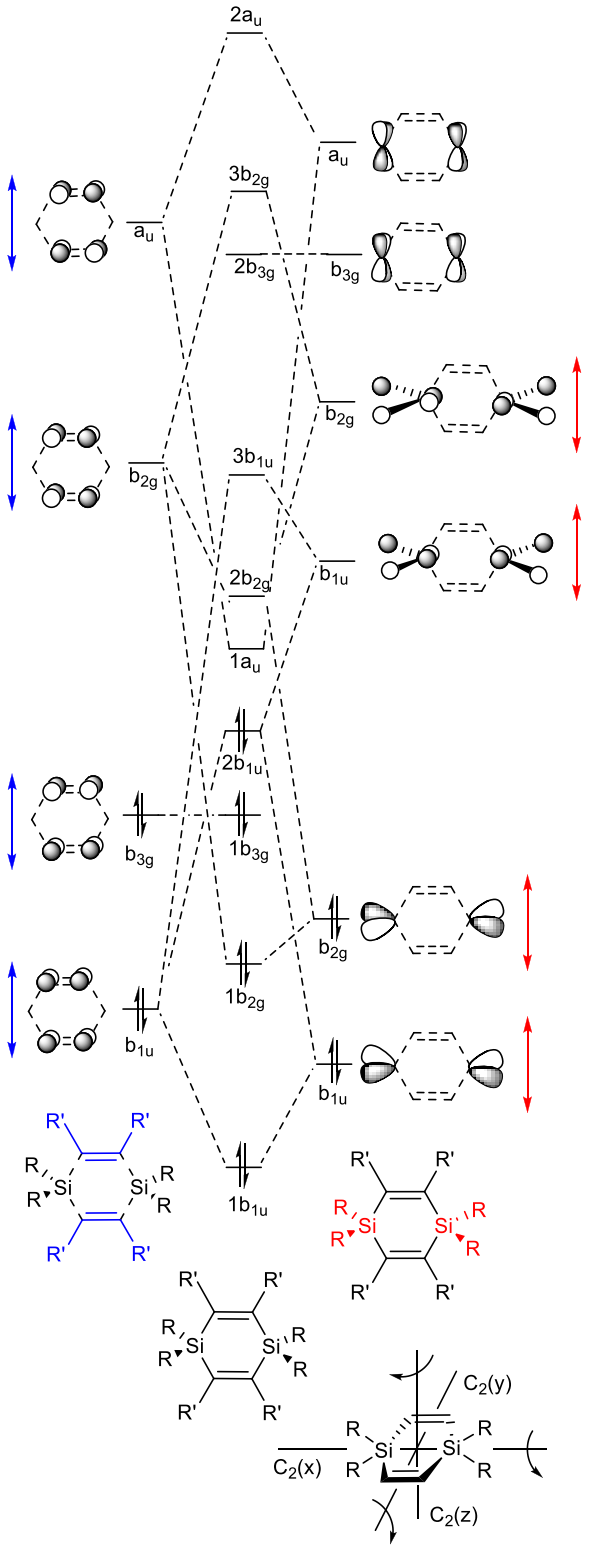

Figure 6. Qualitative molecular orbital (MO) diagram of D_{2h} symmetric 1,4-disilacyclohexa-2,5-diene with the lowest few occupied and unoccupied MOs of π-character constructed from

suitable fragment orbitals. Red arrows indicate changes in fragment orbital energies in dependence of substituents R and blue arrows indicate changes of substituents R'. The orbitals are labelled in accordance with the irreducible representations of the D_{2h} point group. The three C_2 rotational axes are arranged as shown in the structure in the lower right corner.

The energy of MO $2b_{1u}$ will vary depending on the energy of the b_{1u} group orbital of $2x(SiR_2)$ relative to that of the b_{1u} group orbital of 2x(C=C). Thus, the less electronegative R becomes, the higher the energy of this MO will become. The variation in orbital interaction strength can be recognized from the suitable π-symmetry orbitals of 3-hexene and H_2SiR_2. At the B3LYP/6-31G(d) level the π(C=C) of 3-hexene is located at -6.40 eV whereas the $\pi(SiR_2)$ of H_2SiR_2 is found at -11.45 (R = Cl), -8.38 (R = Me), and -6.53 eV (R = TMS) (see Supplementary information for orbital plots). With R = TMS, $2b_{1u}$ can thus be expected to be of particularly high energy, and indeed, this orbital becomes HOMO for **1c** (orbital $2b_1$, Figure 7). The $1b_{3g}$ MO, on the other hand, is not equally affected by the choice of the substituents at Si as it is primarily localized to the C=C bonds. This orbital should instead vary in energy upon a change of substituents R'.

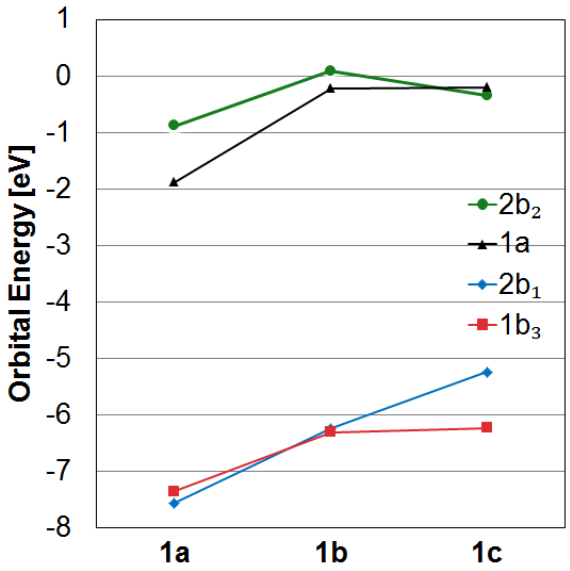

Figure 7. Energy variations of the two occupied frontier molecular orbitals $1b_3$ and $2b_1$ and the two unoccupied frontier orbitals 1a and $2b_2$ of **1a** – **1c** calculated at the B3LYP/6-31G(d) level.

For **1a** – **1c**, the HOMO-1, HOMO, LUMO, and LUMO+1 correspond to either of the $1b_{3g}$, $2b_{1u}$, $1a_u$ and $2b_{2g}$ orbitals of Figure 6, and as the symmetry is reduced from D_{2h} to D_2 the four MOs become $1b_3$, $2b_1$, 1a, and $2b_2$. These four MOs of **1c** are displayed in Figure 8, and which orbital is HOMO ($1b_3$ or $2b_1$) and which one is LUMO (1a or $2b_2$) depends on R (Figure 7). It is noteworthy that no occupied MO with σ-symmetry is found between the $2b_1$ and $1b_3$ orbitals for any of the three compounds. Furthermore, there is a striking similarity of the calculated MOs of **1c** with those of *para*-quinodimethane (**5**, Figure 8) because HOMO-1, HOMO, LUMO, and LUMO+1 of **1c** closely resemble the orbitals of **5** in the order HOMO-1, HOMO, LUMO+1 and LUMO, respectively, *i.e.* LUMO and LUMO+1 change place between the two compounds. Two further items can in particular be noted. First, HOMO of **1c** (-5.24 eV) is nearly isoenergetic to the HOMO of **5** (-5.35 eV) at the B3LYP/6-31G(d) level. Secondly, the a-symmetric orbital which is LUMO+1 in **5** can interact with the a-symmetric group orbital of $2x(SiR_2)$ composed of the two 3d(Si) AOs of **1c**. As a consequence, this MO is lowered in energy so that it becomes the LUMO of **1c**.

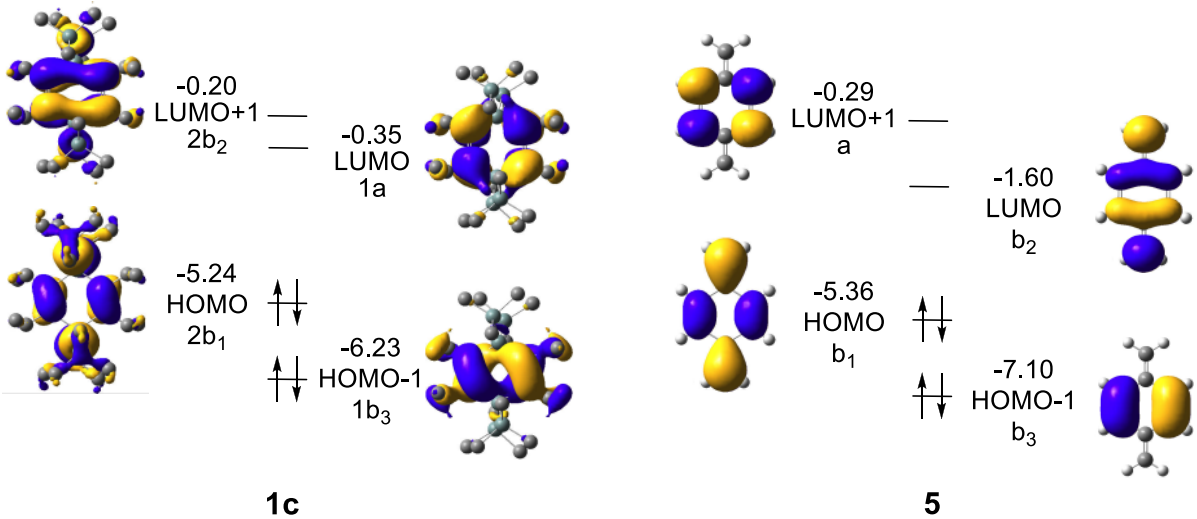

Figure 8. Frontier orbitals, orbital energies in eV, and orbital symmetries of **1c** and *para*-quinodimethane (**5**), as given for the D_2 point group, calculated at the B3LYP/6-31G(d) level. The hydrogen atoms in **1c** are omitted for clarity.

When going from **1a** to **1b**, all four MOs move up in energy with a rather constant amount, but the energy change is slightly larger for the occupied $2b_1$ and the unoccupied $2b_2$ than for $1b_3$ and 1a, reflecting the fact that the first two MOs directly involve the substituents R. However, the most significant change occurs when going from **1b** to **1c** because a large split in the orbital energies of $1b_3$ and $2b_1$ is observed; the latter is raised from -6.24 to -5.24 eV while $1b_3$ merely changes from -6.31 to -6.23 eV. It can furthermore be noted that $1b_3$ has no 3d(Si) AO contribution from 2x(SiR_2), in line with the qualitative MO-diagram of Figure 6.

The LUMO of **1c** also has an interesting character since it is the 1a symmetric MO ($1a_u$ in D_{2h}) which corresponds to an interaction between the a (a_u) symmetric combination of π^*_{CC} at 2x(C=C) with the a (a_u) symmetric combination of the two 3d(Si) AO of 2x(SiR_2) (Figure 6). Hence, this orbital shows that empty 3d(Si) AOs can contribute to the lowest unoccupied MOs when there are suitable local orbitals on adjacent molecular segments to interact with. With a nodal plane coinciding with the SiR_2 plane, the variation in energy of this MO with R is the smallest among the frontier orbitals of Figure **7**. The contribution of 3d(Si) AOs to LUMO is noteworthy because d-AO participation is generally regarded as negligible in the bonding of the heavy main group element compounds in their electronic ground states.[37,38] In contrast, d-orbital participation should play a role for the bonding in the electronically excited states of **1c** in which the LUMO is populated.

Thus, the qualitative MO diagram agrees with the quantitative computations because the $2b_{1u}$ orbital (HOMO of **1b** and **1c** at the B3LYP level) changes substantially in energy by a

change of substituents R. In contrast, the LUMOs do not vary as extensively with R, and for this reason there are large differences in $\Delta\varepsilon_{H\text{-}L}$ between the three compounds, with values of 5.47 (**1a**), 6.03 (**1b**), and 4.89 eV (**1c**) at B3LYP/6-31G(d) level. Taking into account the earlier reported $\Delta\varepsilon_{H\text{-}L}$ of 6.43 eV for the parent species at the same level of computation,[32] one may argue that the 1,4-disilacyclohexa-2,5-diene can be a highly valuable template for extensive variations in electronic and optical properties. Cross-hyperconjugation could be a means for inserting a saturated, yet, conjugated molecular segment into a molecule, allowing for improved physical properties as compared to a purely π-bonded molecule, and at the same time keep the features of a compound with C=C double bonds.

Synthesis: The synthesis of **1a** is based on Jung's procedure in which $HSiCl_3$ and 3-hexyne are heated together with a catalytic amount of Bu_4PCl in a sealed tube, giving **1a** in a yield of 75 % (Scheme 1).[39] However, the reaction was now performed on a five times larger scale than previously reported, and we used a modified approach in which a torch-sealed glass ampoule with the reagents was placed in a steel bomb and heated at 180 °C for 10 hours. Product **1a** was obtained after filtration and distillations. Subsequent addition of four equivalents of MeLi to **1a** gave **1b** in a yield of 75%. 1,4-Disilacyclohexadiene **1c** was formed with a yield of 71% from **1a** with TMSCl and lithium.

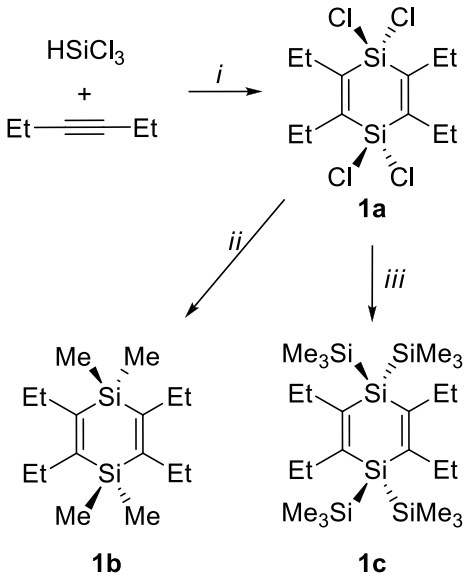

Scheme 1. Reagents and conditions*:* (*i*) Bu_4PCl, 180 °C (sealed tube reaction), 10 hrs, 75%; (*ii*) MeLi, Et_2O, -78 °C to r.t., 12 hrs, 68%; (*iii*) TMSCl, Li, THF, -78 °C to r.t., 13 hrs, 71%.

Geometric structure: The crystal structure of **1c** reveals that this 1,4-disilacyclohexa-2,5-diene adopts a slight twist-chair conformer (**1c-I**, Figure 9) with C_i symmetry and C-Si-C=C dihedral angles within the ring of approximately 13°. The non-planar structure should result from steric repulsion between the ethyl and TMS substituents, and the B3LYP/6-31G(d) calculations reveal that the replacement of the Et groups by smaller Me groups leads from a D_2 to a D_{2h} symmetric molecule with a planar ring. It is noteworthy that a second conformer with the Et groups arranged in an up-down-up-down fashion when starting at the C2-atom following the C2-C3-C5-C6 sequence (conformer **1c-II**, Figure 9) is essentially isoenergetic with **1c-I** when based on the calculated free energy at 298 K. However, using M06-2X, a dispersion corrected DFT method suitable to handle sterically congested molecules, together with the 6-311G(d) basis set indicates that conformer **1c-II** is 2.0 kcal/mol higher in energy than a version of conformer **1c-I** in which the symmetry is reduced from C_i to C_1 (the C_i symmetric conformation of **1c-I** is a second-order saddle point at 0.6 kcal/mol higher energy). Thus, the crystal structure is in accordance with the M06-2X/6-311G(d) calculations. Yet,

both conformers **1c-I** and **1c-II** should be populated at the elevated temperatures of the gas phase UV absorption and UPS spectral measurements (up to 350 °C).

Noteworthy, the calculated B3LYP/6-31G(d) and MP2/6-31G(d) structures of conformer **1c-I** are very similar to the crystal structure and therefore not shown, although selected calculated bond distances and angles are given in the caption of Figure 9. The only notable differences are the B3LYP/6-31G(d) bond lengths, which are slightly longer than the experimental ones, in line with earlier observations.[40]

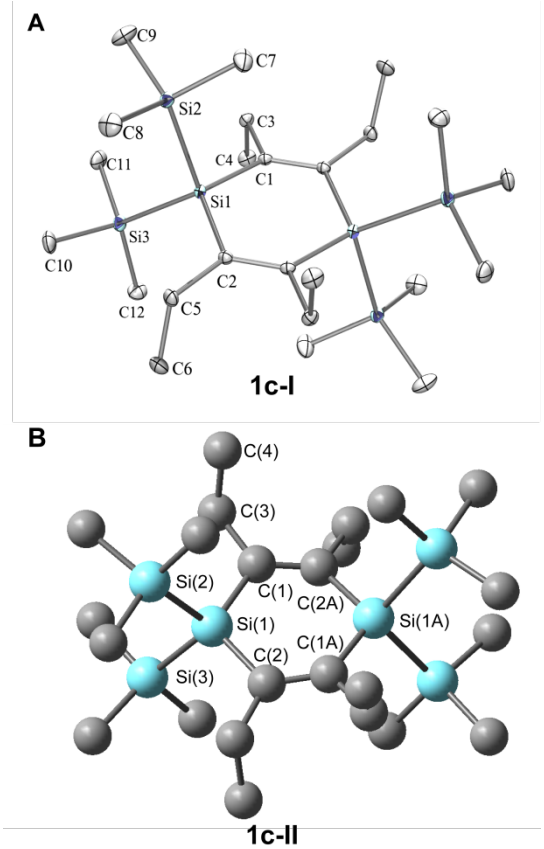

Figure 9. (A) Crystal structure of **1c** (conformer **1c-I**) with the measured data (normal print, for full information see the Supplementary information), and the B3LYP/6-31G(d) calculated data (in italics), and (B) the calculated geometry of the conformer **1c-II** (lower structure, data underlined). Selected bond lengths (Å) and angles (deg), hydrogen atoms omitted for clarity: Si(1)-C(1) 1.8845(13) (*1.907,* 1.905), Si(1)-Si(2) 2.3685(6) (*2.410,* 2.402), Si(1)-Si(3)

2.3690(6) (*2.400,* 2.402), C(1)-C(2A) 1.3456(18) (*1.361,* 1.361), C(1)-C(3) 1.5297(16) (*1.533,* 1.534), C(3)-C(4) 1.5307(19) (*1.5421,* 1.542), Si(2)-Si(1)-Si(3) 109.33(3) (*110.04,* 110.36), Si(1A)-Si(1)-Si(2) 140.33 (*137.06,* 124.82), Si(1A)-Si(1)-Si(3) 110.33 (*112.90,* 124.82), Si(2)-Si(1)-C(1) 113.66(4) (*112.51,* 111.28), Si(3)-Si(1)-C(1) 104.13(4) (*104.67,* 106.21), C(1)-Si(1)-C(2) 111.67 (*111.63,* 111.57), Si(1)-C(1)-C(3) 114.42(9) (*114.96,* 115.28), Si(1)-C(1)-C(2A) 124.05(9) (*123.65,* 123.12), C(1)-Si(1)-C(2)-C(1A) 13.08(14) (*12.11,* 10.82), Si(1)-C(1)-C(2)-Si(1A) 14.71 (*13.54,* 19.83).

The important geometrical parameters for the evaluation of the potential cross-hyperconjugation are the C=C and Si-C bond lengths. A discussion of these bond lengths should, however, be carried out in comparison with those of cross-π-conjugated *para*-quinodimethane **5**. In the X-ray crystal structure of **1c-I** the C=C double bonds (1.346 Å) are slightly longer than ordinary C=C double bonds (1.33 Å),[41] and the Si-C bond lengths (1.885 Å) of the ring are moderately elongated as compared to regular Si-C single bonds (1.87 Å).[42] The elongation of the C=C bonds partially stem from steric congestion between the substituents as revealed through comparisons between the 1,4-disilacyclohexa-2,5-dienes **1d** – **1h** (see Supplementary information), however, there is also a hyperconjugative component that impacts the geometry, and this is revealed through a comparison with **5**. At the B3LYP/6-31G(d) level the C=C double bond lengths of cross-hyperconjugated **1c** are longer than those calculated for the cross-π-conjugated **5** (1.361 vs. 1.349 Å, respectively). Replacement of the ethyl groups (**1g**, Figure **5**) with hydrogen atoms leads to a shortening of the C=C bonds to 1.351 Å, *i.e.*, essentially identical lengths as found for **5**. In contrast, the two isolated C=C bonds in cyclohexa-1,4-diene **6** (1.335 Å) are significantly shorter than in **1g**. The calculated C=C bonds in **1g** are also longer than those of the parent 1,4-disilacyclohexa-2,5-diene (**1h**),

which are 1.344 Å. Thus, the C=C bond elongations observed in **1c** to some extent stem from cross-hyperconjugation. This observation is also true at higher levels of computations because CCSD/6-311G(d) calculations show that **6** has C=C bond lengths of 1.339 Å compared to 1,1,4,4-tetrasilyl substituted **1e** at 1.355 Å and cross-π-conjugated **5** at 1.349 Å.

The most important calculated geometry parameters of **1a** and **1b** are similar to those of **1c**, and for both compounds conformers of type-**I** are more stable than those of type-**II** by 0.4 – 1.0 kcal/mol at B3LYP/6-31G(d) as well as MP2/6-31G(d) levels. For **1a** this relative stability between the two conformer types agrees with the previously determined X-ray crystal structure which was found by Jung and co-workers to correspond to the **1a-I** conformer.[39] The calculated C=C double bonds in both **1a-I** and **1b-I** are minutely shorter than those of **1c-I** (Figure 10). Further discussions and comparisons between the calculated geometries of the 1,4-disilacyclohexa-2,5-dienes **1a** – **1h** are given in the Supplementary Information.

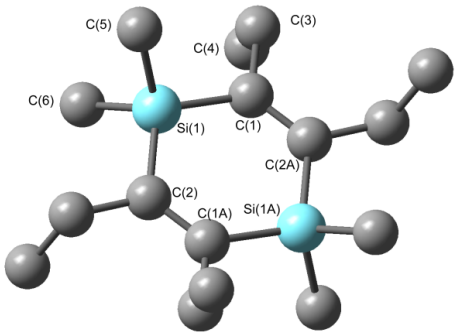

1b-I

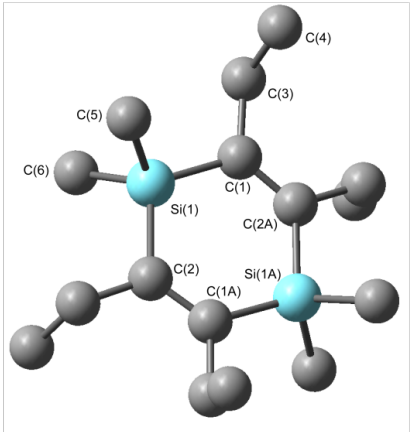

1b-II

Figure 10. Optimized B3LYP/6-31G(d) geometries of **1b-I** (normal print) and **1b-II** (italics). Selected bond lengths (Å) and angles (deg), the hydrogen atoms are omitted for clarity: Si(1)-C(1) 1.890 (*1.891*), Si(1)-C(5) 1.902 (*1.903*), Si(1)-C(6) 1.903 (*1.903*), C(1)-C(2A) 1.357 (*1.358*), C(2)-C(5) 1.531 (*1.532*), C(3)-C(4) 1.542 (*1.542*), C(7)-Si(1)-Si(6) 106.54 (*106.90*), Si(1A)-Si(1)-C(5) 132.65 (*131.77*), Si(1A)-Si(1)-C(6) 120.80 (*121.33*), C(5)-Si(1)-C(1) 110.56 (*110.42*), C(6)-Si(1)-C(1) 107.77. (*110.14*), C(5)-Si(1)-C(6) 113.33 (*112.98*), Si(1)-C(1)-C(3) 114.92 (*115.43*), Si(1)-C(1)-C(2A) 123.02 (*123.43*), C(1)-Si(1)-C(2)-C(1A) 9.74 (*1.00*), Si(1)-C(1)-C(2)-Si(1A) 8.88 (*9.01*).

Photoelectron spectroscopy: The experimental verification of the substituent effect on the electronic structures of 1,4-disilacyclohexa-2,5-dienes comes through photoelectron and UV absorption spectroscopies, as well as through cyclic voltammetry. The cationic valence electronic states of **1b** and **1c** were studied by conventional photoelectron spectroscopy using HeIα radiation at hν = 21.22 eV for ionization. Interpretation of the spectra were made on the basis of outer valence Green's function (OVGF) calculations at the OVGF/6-311+G(d)//B3LYP/6-31G(d) level. The D_2 symmetric conformers **1b-II** and **1c-II** were used to facilitate rationalization in terms of qualitative MO-theory. The ionization energies of the C_i symmetric conformers **I** differ minutely, and tables which enable comparisons between conformers **I** and **II** are given in the Supplementary information.

With regard to **1b**, the valence photoelectron spectrum shows a well-defined onset at 7.9 eV followed by broad rounded bands (see Figure 11). The computed energies group around the spectral features so that a rather good understanding is achievable despite the strong overlap of bands. The experimental and calculated energies for the lower states are summarized in Table 1 along with our interpretations (for a complete table see the Supplementary information).

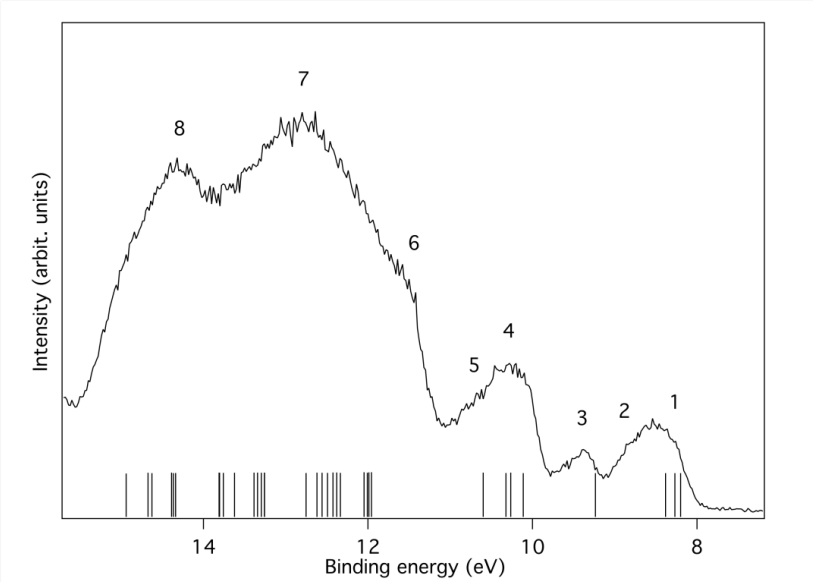

Figure 11. The photoelectron spectrum of 1,1,4,4-tetramethyl-2,3,5,6-tetraethyl-1,4-disilacyclohexa-2,5-diene (**1b**) excited using HeIα radiation at 21.22 eV. The bands are numbered as in Table 1. Ionization energies calculated at the OVGF/6-311+G(d)//B3LYP/6-31G(d) level are included as bars on the energy axis.

Table 1. Experimental (peak maximum from the photoelectron spectrum) and calculated binding energies (eV),[a] with assignments (term) of **1b** with D_2 symmetry (1b-II conformer)

Structure number	Binding energy (exp)	Binding energy (calc)	Assignment (orbital type)	Comment
1	7.9			Onset
1	8.5	8.20	b_1 (π)	Peak max
		8.27	b_3 (π)	Peak max

2	8.9	8.38	b_1 (σ)	Shoulder
3	9.4	9.24	b_3 (σ)	Peak max
4	10.3	10.11	a (σ)	Peak max
		10.26	b_2 (π)	
		10.32	b_2 (σ)	
5	10.7	10.60	b_1 (π)	Shoulder

Calculated at ROVGF/6-311+G(d)//B3LYP/6-31G(d) level.

The first band with a peak maximum at 8.5 eV represents ionization from three different orbitals that are close in energy according to the computations. The two lowest of these have b_1 and b_3 symmetries, in line with the qualitative MO-diagram of Figure 6. The splitting is rather small (70 meV) and the $2b_1$ MO is found above the $1b_3$ MO. It can also be noted that the first ionization energy of **1b** is similar to those earlier reported for 2,3-dimethyl-2-butene and **6** (8.4 and 8.8 eV, respectively).[43,44] The third orbital expected to give rise to appreciable intensity in this band is a b_1 symmetric σ-type orbital composed of in-plane p and s atomic orbitals located on both the C and Si atoms of the ring, and it is slightly shifted to higher binding energy compared to the π-type orbitals. It can also tentatively be connected to the formation of the shoulder on the high binding energy side of the band. An angle resolved study could presumably confirm the assignment since the beta value distribution of σ-orbitals is normally rather different from that of π-orbitals. The band at 9.4 eV, assigned to feature 3 in the spectrum, is connected to one single σ-orbital with b_3 symmetry.

The third band with a peak maximum at 10.3 eV is connected to ionization from four different orbitals, pair-wise similar of π-and σ-symmetry, respectively. The former two can be

characterized essentially as in-phase (b_1) and out-of-phase (b_2) combinations of the two $\pi(SiMe_2)$ group orbitals (*cf*. Figure 6). The b_1 symmetric MO also has some contribution from π(C=C), and the calculated energy separation between the two resulting MOs is 0.34 eV.

The pressure that could be obtained in the ionization chamber for **1c** was much lower than for **1b**, and the recording of the spectrum was very time-consuming. Due to these experimental constraints we recorded the spectral region between 5.5 eV and 9.5 eV several times and summed the individual spectra (Figure 12). However, the region above 9.5 eV was included in only one of the recordings. The statistics is therefore not as good as for **1b**, in particular in the higher binding energy region where signals from remaining H_2O and N_2 in the spectrometer are present. Yet, in the lower energy range the spectrum seems to be free of such influences. Some broad structures can be identified in this part, and their energies are given along with orbital characters in Table 2.

The first band is located at 7.1 eV (peak maximum), and according to the calculations it corresponds to the ionization from a single π-orbital of b_1 symmetry. It should particularly be noted that the energy is substantially lower than for any orbital of **1b**, suggesting that the influence of the $SiMe_3$ substituent character is significant. Thus, in line with the MO-theoretical description of Figure 6, the $Si(SiMe_3)_2$ segment provides local $\pi(ER_2)$ orbitals which are matched energetically with the π-orbitals of the 2x(C=C) fragment, pushing up the MO which is the out-of-phase combination of the b_1 symmetric group orbitals of the 2x(C=C) and 2x(SiR_2) segments when compared to **1b**. This confirms experimentally the large energy difference between HOMO and HOMO-1 of **1c**, as compared to **1a** and **1b**, observed in the B3LYP calculations (*cf*. Figure 7).

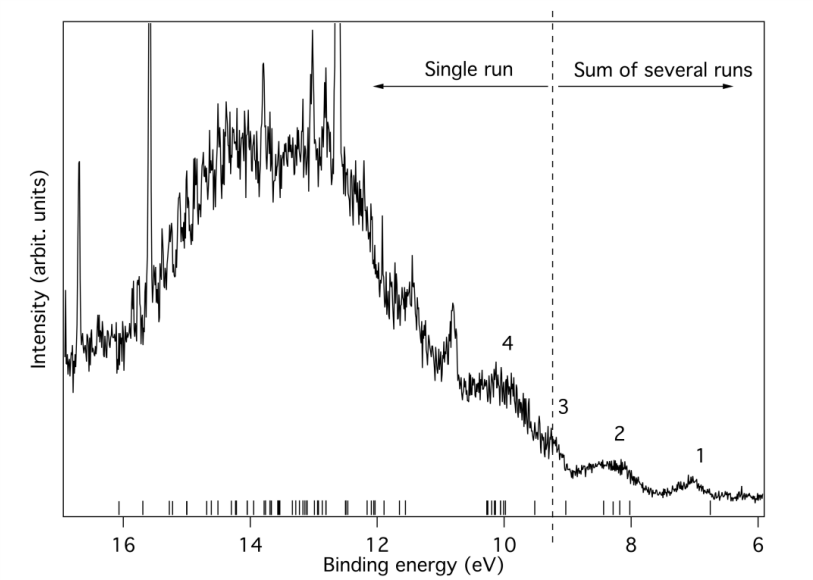

Figure 12. The photoelectron spectrum of 1,1,4,4-tetrasilyl-2,3,5,6-tetraethyl-1,4-disilacyclohexa-2,5-diene (**1c**) excited using HeIα radiation at 21.22 eV. The bands are numbered in accordance with Table 2. Ionisation energies calculated at the OVGF/6-311+G(d)//B3LYP/6-31G(d) level are included as bars on the energy axis.

Table 2. Experimental (peak maximum from the photoelectron spectrum) and calculated binding energies (eV) with assignments (term) of the **1c** molecule with D_2 symmetry (**1c-II**).

Structure number	Binding energy (exp)	Binding energy (OVGF)	Assignment (orbital type)	Comment
1	6.7			Onset
	7.1	6.76	b_1 (π)	Peak max
2	7.6			Onset
	8.3	8.02	b_3 (π)	
		8.18	b_2 (π)	
		8.28	b_1 (σ)	

		8.43	b_3 (σ)
3	9.3	9.03	a (σ)
		9.52	b_1 (π)
		9.98	b_2 (σ)

[a] Calculated at the ROVGF/6-311+G(d)//B3LYP/6-31G(d) level.

The second band is broader and stronger, indicating ionization from more than one orbital. The peak maximum is observed at approximately 8.3 eV, and the calculations put four orbitals in this energy range. These orbitals are mostly of π-character and primarily located on the ring. The photoelectron band is therefore expected to resemble the outermost band of **1b**, both in energy and general shape, due to the mutual similarity between the orbitals. This similarity is indeed observed as seen in Figure 13 where the lower binding energy region of the photoelectron spectra of **1b** and **1c** are shown in comparison to the numerical results. The most notable difference is the energy for ionization from the HOMO in the two compounds.

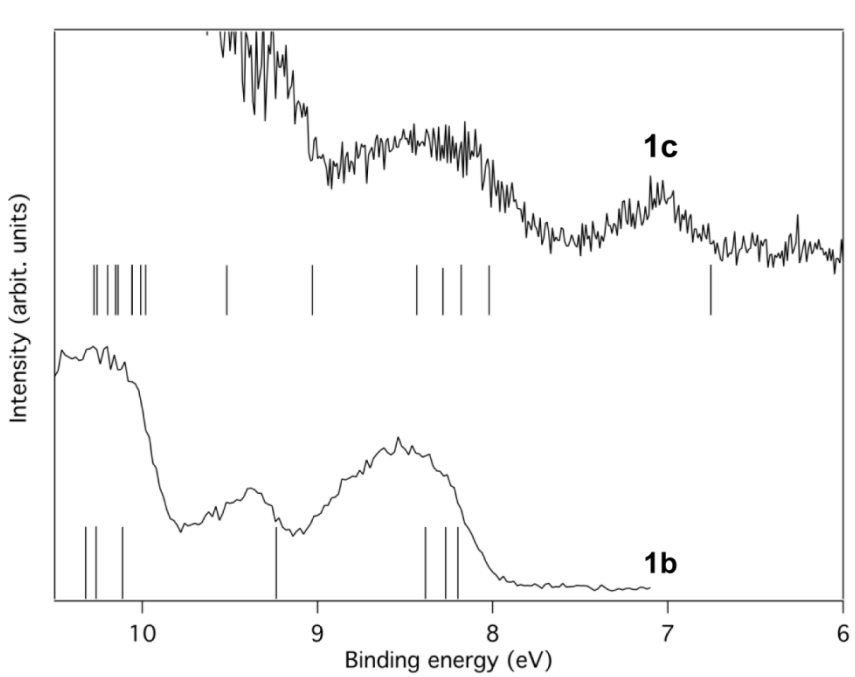

Figure 13. A comparison of the lower binding energy regions of the photoelectron spectra of **1b** and **1c** excited using HeIα radiation at 21.22 eV. Ionisation energies calculated at the OVGF/6-311+G(d)//B3LYP/6-31G(d) level are included as bars on the energy axis.

Cyclic voltammetry: To provide further evidence for the role of the substituents on the frontier orbital energies, compounds **1a - 1c** were investigated by cyclic voltammetry. Figure 14 displays the anodic scan of compounds **1a** (black), **1b** (blue) and **1c** (red). All three compounds show electrochemically irreversible oxidation processes at 1.47, 0.88 and 0.46 V vs. Fc/Fc^{+}, respectively. Thus, the oxidative peak potential of **1c** is cathodically shifted by 400 mV compared to that of **1b** and by 1 V relative to **1a**. These findings strongly support the results obtained in the UPS spectroscopy as well as in the computational studies. The findings also hint to extensive variations in redox properties that could be useful for future applications.

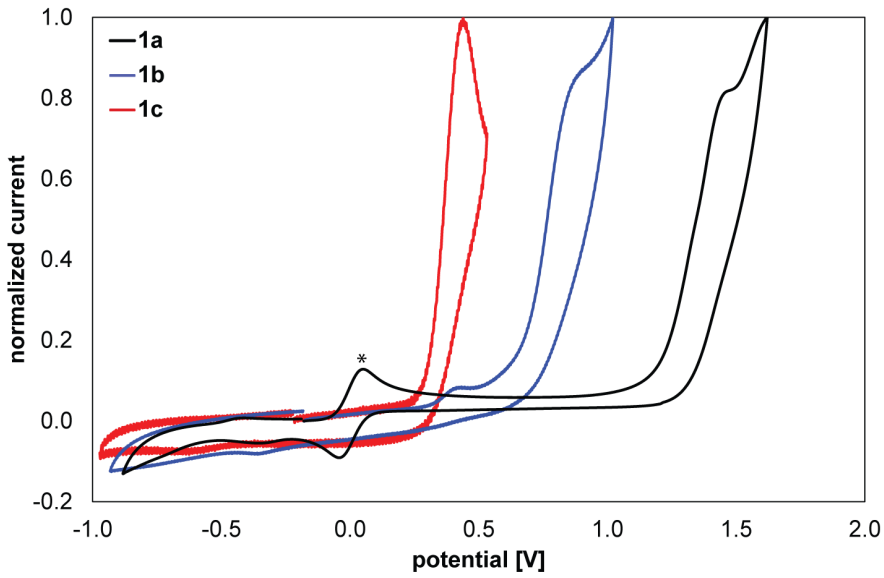

Figure 14. Cyclic voltammograms (anodic scans) of **1a** (black)**, 1b** (blue), **1c** (red) (1mM solutions in CH_2Cl_2) containing 0.1 M NBu_4PF_6 vs. $Fc^{+/0}$, v = 200 mV/s. * Fc^{+}/Fc^{0} couple as internal standard.

UV absorption spectroscopy: The electronic excitation energies of the three 1,4-disilacyclohexa-2,5-dienes **1a** – **1c** and cyclohexa-1,4-diene **6** were recorded by gas phase UV absorption spectroscopy (Figure 15), as described in the experimental section below. The wavelengths and extinction coefficients at the absorption peaks are summarized in Table 3 - 5. The UV absorption spectra of **1a** and **1b** were only recorded in the gas phase as solvent interferences when recorded in cyclohexane were so strong that no reliable spectral information was obtained. For **1c**, both gas phase and solution spectra were recorded, and the gas phase measurement clearly reveals a thermal redistribution of the curve as compared to the measurement at room temperature in cyclohexane, a result of vibrational broadening.

Compounds **1a** and **1b** have similar characteristics as their spectra are composed of two overlapping bands; one centered at 210 – 220 nm and the second in the range 190 – 200 nm. The strongest absorptions are found in the lower wavelength range (198 and 196 nm for **1a** and **1b**, respectively). 1,4-Disilacyclohexa-2,5-diene **1c**, on the other hand, shows notably different spectral features, with the most intriguing feature being the strong absorption at 273 nm (4.55 eV). A comparison with the UV absorption spectrum of cyclohexa-1,4-diene (**6**) further reveals the difference between the SiR_2 and CH_2 units as mediators between the two C=C bonds because **6** does not absorb above 220 nm. Moreover, the molecular extinction coefficients of the excitations of **6** are much smaller than for the excitations of any of the three 1,4-disilacyclohexa-2,5-dienes.

In **1c**, two weakly chromophoric trisilane segments have been incorporated, and it is apparent from the UV spectrum that these couple strongly with the two C=C bonds because the first absorption of permethylated trisilane, Si_3Me_8, has been reported at 216 nm (5.75 eV).[45] Hence, the chromophore of **1c** constitutes the complete cycle involving the two C=C bonds and the two trisilane segments.

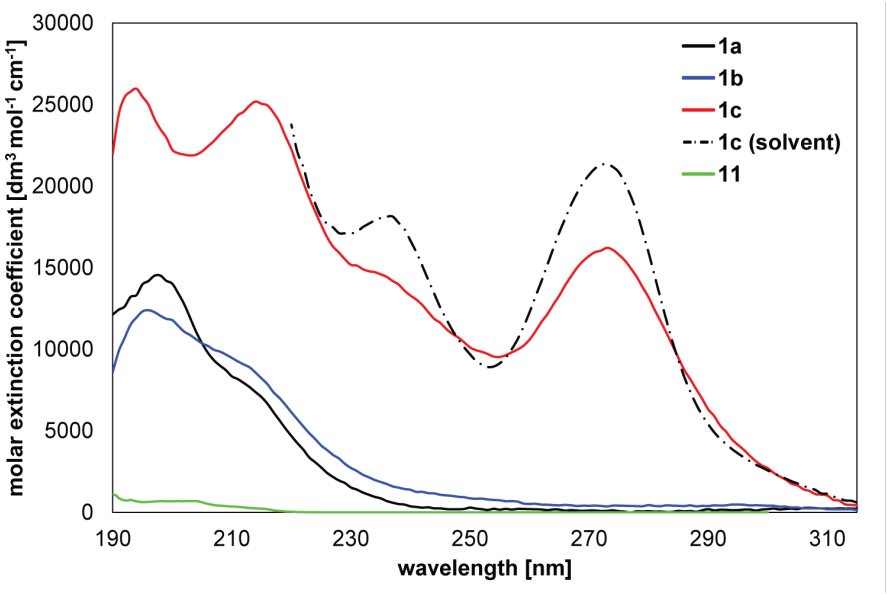

Figure 15. UV absorption spectra of **1a** (black), **1b** (blue), **1c** (red), and **11** (green) recorded in gas phase, and for **1c** also the spectrum recorded at room temperature in cyclohexane solution (black dashed curve). The temperature gradients for **1a** and **1b** went from 240 °C (bottom) to 340 °C (top), and for **1c** from 250 °C at the bottom to 350 °C at the top. The gas phase UV absorption measurement of **6** was performed at room temperature. For further details on the UV measurements see the Supplementary information.

In order to analyze the experimental UV absorption spectra, excitation energies and oscillator strengths were calculated using time-dependent DFT (TD-DFT) at the TD-PBE0/6-31+G(2d)//B3LYP/6-31G(d) level (Table 3 - 5). To allow for a facile comparison with the D_{2h} symmetric **5** we discuss the type-**II** conformers for all three compounds, although both conformers **I** and **II** will be nearly equally populated at the elevated temperatures used. The calculated excitation energies and oscillator strengths of conformer **I** closely resembles those of conformer **II** (for full comparison between conformer types **I** and **II**, see the Supplementary information). In general, the calculated excitation wavelengths (energies) of the three compounds **1a-II** to **1c-II** agree with the recorded values of Figure 15.

The first calculated transition of **1a-II**, which is dark and of B_3 symmetry, appears at 262 nm (4.74 eV) and involves excitations from HOMO-1 and HOMO-2 to LUMO (see Supplementary information). The second calculated transition, which also is dark but of B_1 symmetry, is calculated at 253 nm (4.89 eV) and it is the transition that most clearly corresponds to an excitation from HOMO to LUMO. The first transition with a significant calculated oscillator strength is of B_3 symmetry and it is found at 231 nm (5.37 eV), likely corresponding to the shoulder at ~220 nm in the experimental spectrum. The strongest allowed transition (B_3 symmetry) is found at 198 nm and calculated at 203 nm (6.09 eV). This transition has a substantial contribution of HOMO to LUMO+1 excitation. In particular, it is noteworthy that all allowed transitions of **1a-II** are of B_3 symmetry.

The first calculated transition of **1b-II** found at 240 nm is of B_3 symmetry and weakly allowed. Indeed, a longer tail towards longer wavelengths is observed in the experimental spectrum of **1b** than in that of **1a** (Figure 15). The first strong transition according to the calculations is the fourth transition (B_3 symmetric) with a λ_{max} of 226 nm (5.48 eV), which together with the weakly allowed fifth transitions at 220 nm (5.64 eV, B_1 symmetric), and the sixth transition at 212 nm (5.84 eV, B_3 symmetric) should represent the shoulder in the UV absorption spectrum at ~215 nm. This shoulder occurs at a similar position as for **1a**. Yet, the most visible transition in the experimental spectrum occurs at 196 nm (6.33 eV) and is of B_3 symmetry according to the computations. This transition is, however, difficult to interpret in terms of excited configurations.

The most interesting spectrum among the 1,4-disilacyclohexa-2,5-dienes studied is displayed by **1c**. Its first calculated excitation is a dark transition at 311 nm (3.98 eV) of B_1 symmetry and it has significant character of an excitation from HOMO to LUMO (*cf* Figure 8). However, the second excitation calculated at 276 nm (4.50 eV) is strongly allowed and of B_3 symmetry. This transition should correspond to the strong peak observed experimentally at

273 nm and it has a strong contribution of the HOMO to LUMO+1 excitation, but also of the HOMO-1 to LUMO excitation. As the transition has strong HOMO to LUMO+1 excitation character, *i.e.*, a transition between the two MOs which have clear cross-hyperconjugative character involving both trisilane and olefin fragments, this transition can only be observed in **1c** and closely related 1,4-disilacyclohexadiene derivatives. In the wavelength range 230 – 240 nm there is a clear, yet slightly weaker transition which should correspond to the B_3 symmetric transition calculated at 229 nm (5.41 eV). According to TD-DFT this state has no simple description in terms of excited configurations. The last calculated strong visible transition above 200 nm (6.21 eV) is found at 214 nm and the calculations give a B_3 symmetric transition at 222 nm (5.58 eV). Finally, the experiments reveal a strong transition at 196 nm (6.33 eV), but this excitation was not calculated as it is less than 1 eV from the first ionization energy of **1c** making the computed excitation dubious.

We also examined the emissive properties of **1c** but no emission could be detected upon excitation at 273 nm. However, **1c** also does not photodecompose when irradiated with $\lambda >$ 220 nm light, indicating that non-radiative pathways bring it back to the electronic ground state. In contrast, a rapid photodegradation, potentially due to silylene extrusion from the trisilane segments, is observed upon irradiation at shorter wavelengths than 220 nm.

Table 3. Gas phase UV spectral data compared with calculated[a] values of **1a.**

Exp [nm]	ε [$dm^{-3}mol^{-1}\,cm^{-1}$]	Calc. [nm (eV)]	Sym. (D_2)	*f*
-	-	262 (4.72)	B_3	0.002
-	-	253 (4.89)	B_1	0.007
(220)	-	231 (5.36)	B_3	0.115
-	-	225 (5.51)	B_1	0.025

-	-	208 (5.95)	A	0.000
-	-	205 (6.05)	B_1	0.001
198	14500	203 (6.09)	B_3	0.485
-	-	202 (6.11)	B_1	0.018
-	-	199 (6.22)	A	0.000
-	-	198 (6.25)	B_2	0.040
-	-	195 (6.35)	B_3	0.091

[a] TD-PBE0/6-31+G(2d)//B3LYP/6-31G(d)

Table 4. Gas phase UV spectral data compared with calculated[a] values of **1b**.

Exp [nm]	ε [$dm^{-3}mol^{-1}\,cm^{-1}$]	Calc. [nm (eV)]	Sym. (D_2)	*f*
-	-	240 (5.16)	B_3	0.015
-	-	232 (5.35)	B_1	0.008
-	-	227 (5.46)	B_1	0.004
-	-	226 (5.48)	B_3	0.067
-	-	220 (5.63)	B_1	0.023
(215)	-	212 (5.84)	B_3	0.326
-	-	206 (6.02)	B_1	0.011
-	-	201 (6.16)	B_1	0.026
-	-	199 (6.22)	B_3	0.091
-	-	199 (6.23)	B_2	0.002
-	-	197 (6.30)	B_1	0.002
-	-	197 (6.30)	A	0.000
196	12400	196 (6.33)	B_3	0.114

[a] TD-PBE0/6-31+G(2d)//B3LYP/6-31G(d)

Table 5. Gas phase UV spectral data compared with calculated[a] values of **1c**.

Exp [nm]	ε [$dm^{-3}mol^{-1}$ cm^{-1}]	Calc. [nm (eV)]	Sym.	*f*
-	-	311 (3.98)	B_1	0.000
273	16200	276 (4.49)	B_3	0.356
-	-	254 (4.87)	B_1	0.039
-	-	252 (4.92)	B_3	0.016
-	-	247 (5.03)	B_1	0.000
-	-	246 (5.03)	B_3	0.019
-	-	243 (5.10)	B_2	0.002
-	-	241 (5.13)	A	0.000
-	-	241 (5.15)	B_1	0.019
-	-	235 (5.28)	A	0.000
-	-	233 (5.33)	B_2	0.046
-	-	230 (5.39)	B_1	0.031
(237)	18100	229 (5.41)	B_3	0.138
-	-	224 (5.54)	B_2	0.002
-	-	223 (5.55)	B_3	0.001
214	25200	222 (5.58)	B_3	0.381
-	-	221 (5.62)	B_1	0.000
-	-	220 (5.63)	B_2	0.017
-	-	219 (5.65)	B_3	0.000

-	-	219 (5.66)	A	0.000
-	-	215 (5.77)	B_1	0.000
-	-	215 (5.78)	A	0.015
-	-	212 (5.86)	A	0.013
-	-	211 (5.88)	B_1	0.000
-	-	210 (5.90)	B_3	0.024
-	-	208 (5.96)	B_1	0.008
-	-	207 (5.99)	A	0.000
-	-	203 (6.10)	B_3	0.024
-	-	203 (6.10)	B_2	0.008
196	26000			

[a] TD-PBE0/6-31+G(2d)//B3LYP/6-31G(d)

[b] Calculated peaks are reported until 6.10 eV, *i.e.*, 1.00 eV below the first ionization peak at 7.10 eV according to our photoelectron spectrum of **1c**.

***On the impact of cyclic cross-hyperconjugation in 1c*:** To determine the importance of the cyclic nature of cross-hyperconjugation in **1c** *vs* linear hyperconjugation and acyclic cross-hyperconjugation we calculated the UV absorption and electron binding energies for a series of additional compounds (**7** – **10**, Figure 5) at TD-PBE0/6-31+G(2d)//B3LYP/6-31G(d) and OVGF/6-311+G(d)//B3LYP/6-31G(d) levels (results of additional TD-M06-2X/6-31+G(2d)//B3LYP/6-31G(d) calculations is found in the Supplementary Information). The tetra ethyl analogue of one of these compounds, **7**, could at first glance be generated experimentally through hydrogenation of **1c**. However, despite numerous attempts using different conditions we were unable to reduce any of the double bonds in **1c**, presumably due to the extensive steric bulk of the four ethyl and four TMS substituents.

Computations of **1g**, the derivative of strongly cross-hyperconjugated **1c** with the ethyl groups replaced by hydrogens reveal that the ethyl groups have only a small effect on the electronic structure of **1c** (first excitations at 299 and 311 nm (4.16 and 3.98 eV) for **1g** and **1c**, respectively) and a moderate effect on the first binding energy (7.14 and 6.76 eV, respectively). Replacing one of the C=C double bonds by a saturated C-C bond to yield **7**, rendering this compound linearly hyperconjugated, results in a significant change in the calculated UV absorption spectra with the first transition at 263 nm (4.71 eV) and a first binding energy of 7.76 eV. Breaking the cyclic nature of the cross-hyperconjgation by replacing one of the $Si(SiMe_3)_2$ groups with a CH_2 group, yielding the acyclic cross-hyperconjugated **8**, has a similar large effect leading to a first transition at 261 nm (4.75 eV) and a first binding energy of 7.53 eV. Replacing one of the C=C double bonds of **8** with a saturated C-C bond leading to **9**, with a short linearly hyperconjugated path, gives a compound which is less hyperconjugated according to the TD-DFT and OVGF results (first transition at 236 nm (5.25 eV), binding energy 7.77 eV). Finally, replacing both the double bonds of **1g** with saturated C-C bonds results in a compound, **10**, with two isolated $Si(SiMe_3)_2$ segments. This compound has experimentally been found to not absorb above 220 nm in accordance with computations.[46]

Taken together, 1,4-disilacyclohexadiene **1c** clarifies that neutral cyclic cross-hyperconjugation can be used similarly as regular cyclic cross-π-conjugation, and that a $Si(SiMe_3)_2$ moiety can replace an exocyclic C=C double bonded segment in a conjugated molecule. This finding should provide for new opportunities for the design of optically and electronically active compounds.

Conclusions

1,4-Disilacyclohexa-2,5-dienes are a compound class that allows for remarkable variations in the electronic and optical characteristics through the choice of the substituents. Herein, the effects of the substituents R at the two silicon atoms (R = Cl (**1a**), Me (**1b**), or $SiMe_3$ (**1c**)) on the valence photoionizations energies, the first oxidation potentials, and the lowest UV absorption energies have been analyzed. The cause of the large tunability stems from the fact that the two SiR_2 segments when incorporated in the cyclic cyclohexa-1,4-diene fragment allow for neutral cyclic cross-hyperconjugation to various degrees. A strong cyclic cross-hyperconjugation is found with R = $SiMe_3$ and much weaker when R = Cl and Me. One can predict that a change of the substituents at the C=C double bonds provides for further tuning of the electronic and optical properties, as suggested by the results of the 1,4-disilacyclohexa-2,5-diene with the 2,3,4,5-tetraethyl substituents replaced by hydrogens. Thus, it is likely that even larger variations in the spectral properties than those reported herein can be achieved.

Among **1a** – **1c**, valence photoelectron spectroscopy shows that **1c** has the lowest binding energy of ~ 7.1 eV, *i.e.*, about 1.4 eV lower than that of **1b**. The cyclic voltammograms of **1a** – **1c** show substantial differences in the observed oxidation potentials. Compound **1c** features the lowest oxidation potential, while those of **1a** and **1b** are anodically shifted by 400 mV and 1 V, respectively. Gas phase UV absorption spectroscopy of **1c** reveals a strong absorption at 273 nm (4.55 eV), whereas compounds **1a** and **1b** have no strongly allowed excitations above 215 nm (below 5.77 eV). The neutral cross-hyperconjugation strengths in these compounds were clarified with quantum chemical calculations combined with a MO-theoretical analysis. Interestingly, the orbital pattern and the electronic structure of **1c** has similarities with that of the cross-π-conjugated *para*-quinodimethane (**5**). The 1,4-disilacyclohexa-2,5-diene is therefore a new monomer unit which in an optimal way combines σ- and π-bonded segments into a rigid neutral hyperconjugated framework. It should represent an interesting structural motif for new molecules with applications in the molecular and organic electronics areas.

Acknowledgements

We thank Dr. Carla Puglia for many valuable discussions. We are grateful for financial support from the Swedish Research Council, from Uppsala University for the U^{3}MEC KoF07 Initiative, from the Wenner-Gren Foundations in the form of a postdoctoral fellowship to A.W., and from the Göran Gustafsson Foundation (S.O and D.N.). The National Supercomputer Center (NSC) in Linköping, Sweden is acknowledged for a generous allotment of computer time.

Supplementary information

Electronic Supplementary information (ESI) includes: Full computational and experimental procedures as well as details on the gas phase UV absorption spectroscopy, analysis of the impact of steric and electronic factors on the geometries of 1,4-disilacyclohexa-2,5-dienes **1a** – **1h**, orbital plots, absolute electronic energies, Cartesian coordinates, tables with TD-DFT data, tables with complete photoelectron spectroscopic data and X-ray crystallographic information for compound **1c.**

Notes and references

1 See complete volume *Chem. Rev.*, 2005, **105**, 3433–3947.

2 (a) R. D. Miller and J. Michl, *Chem. Rev.*, 1989, **89**, 1359–1410; (b) J. Michl and R. West, *Acc. Chem. Res.*, 2000, **33**, 821– 823.

3 T. A. Skotheim and J. R. Reynolds, *Handbook of Conducting Polymers*; CRC Press LLC, Bocata Raton, 2007.

4 (a) R. S. Mulliken, *J. Chem. Phys.*, 1939, **7**, 339–352; (b) R. S. Mulliken,C. A. Rieke and W. G. Brown, *J. Am. Chem. Soc.*, 1941, **63**, 41–56; (c) I. V. Alabugin and T. A. Zeidan,

J. Am. Chem. Soc., 2002, **124**, 3175–3185; (d) J. B. Lambert and R. A. Singer, *J. Am. Chem. Soc.*, 1992, **114**, 10246; (e) I. V. Alabugin, K. M. Gimore and P. W. Peterson, *WIREs Comput. Mol. Sci*., 2011, **1**, 109–141.

5 We use the term cross-hyperconjugation instead of hypercross-conjugation to stress that the geminal connectivity of the conjugated paths should have higher priority than the specific conjugation type.

6 For recent reviews in silole-containing oligomers and polymers see, e.g.: (a) K. Tamao and S. Yamaguchi, *J. Organomet. Chem.*, 2000, **611**, 5–11; (b) S. Yamaguchi and K. Takao, *J. Organomet. Chem.*, 2002, **653**, 223–228; (c) S. Yamaguchi and K. Tamao, *Chem. Lett.*, 2005, **34**, 2; (d) J. Chen and Y. Cao, *Macromol. Rapid Commun*., 2007, **28**, 1714–1742; (e) J. Ohshita, *Macromol. Chem. Phys.*, 2009, **210**, 1360–1370.

7 (a) M. Nakamoto, Y. Inagaki, M. Nishina and A. Sekiguchi, *J. Am. Chem. Soc.*, 2009, **131**, 3172–3173; (b) T. Ochiai, M. Nakamoto, Y. Inagaki and A. Sekiguchi, *J. Am. Chem. Soc.*, 2011, **133**, 11504-11507; (c) Y. Inagaki, M. Nakamoto and A. Sekiguchi, *J. Am. Chem. Soc.*, 2011, **133**, 16436–16439; (d) A. Chrostowska, A. Dargelos, P. Baylère, A. Graciaa, Y. Inagaki, M. Nakamoto, V. Ya Lee and A. Sekiguchi, *ChemPlusChem*, 2013, **78**, 398–401.

8 R. Emanuelsson, A. Wallner, E. A. M. Ng, J. R. Smith, D. Nauroozi, S. Ott and H. Ottosson, *Angew. Chem. Int. Ed. Engl.*, 2013, **52**, 983–987.

9 U. Weidner and A. Schweig, *Angew. Chem. Int. Ed. Engl*., 1972, **11**, 536–537.

10 (a) R. Hoffmann, *Act. Chem. Res.*, 1971, **4**, 1–9; (b) R, Srinivasan, L. S. White, A. R. Rossi and G. A. Epling, *J. Am. Chem. Soc*., 1981, **103**, 7299– 7304.

11 M. Ishikawa and J. Ohshita, in *Organic Conductive Molecules and Polymers*, Ed.: H. S. Nalwa, Ch. 30, Wiley, New York, 1997.

12 J. Ohshita and A. Kunai, *Acta Polym.* 1998, **49**, 379–403.

13 J. Ohshita, H. Takata, H. Kai, A. Kunai, K. Komaguchi, M. Shiotani, A. Adachi,K. Sakamaki, K. Okita, Y. Harima, Y. Kunugi, K. Yamashita and M. Ischikawa, *Organometallics*, 2000, **19**, 4492–4498.

14 J. Ohshita, M. Hashimoto, K. –H. Lee, H. Yoshida and A. Kunai, *J. Organomet. Chem.*, 2003, **682**, 267–271.

15 J. Ohshita, D. –H. Kim, Y. Kunugi and A. Kunai, *Organometallics*, 2005, **24**, 4494–4496.

16 D. –H. Kim, J. Ohshita, T. Kosuge, Y. Kunugi and A. Kunai, *Chem. Lett.*, 2006, **3**, 266–267.

17 J. Ohshita, Y. Izumi, D.–H. Kim, A. Kunai, T. Kosuge, Y. Kunugi, A. Naka and T. Ishikawa, *Organometallics*, 2007, **26**, 6150–6154.

18 J. Ohshita, Y. Hatanaka, S. Matsui, T. Mizumo, Y. Kunugi, Y. Honsho, A. Saeki, S. Seki, J. Tibbelin, H. Ottosson, and T. Takeuchi, *Dalton Trans.*, 2010, **39**, 9314–9320.

19 J. Ohshita, Y. Hatanaka, S. Matsui, Y. Ooyama, Y. Harima and Y. Kunugi, *Appl. Organomet. Chem.*, 2010, **8**, 540–544.

20 Y. Yamaguchi, *Synth. Met.*, 1996, **82**, 149–153.

21 S. Yamaguchi and K. Tamao, *Bull. Chem. Soc. Jpn.*, 1996, **69**, 2327–2334.

22 S. Yamaguchi. R.–Z. Jin and K. Tamao, *Organometallics*, 1997, **16**, 2486–2488.

23 K. –I. Kanno, M. Ichinohe, C. Kabuto and M. Kira, *Chem. Lett.,* 1998, **1**, 99–100.

24 S. Yamaguchi, R. –Z. Jin and K. Tamao, *J. Am. Chem. Soc.* 1999, **121**, 2937–2938.

25 R. West, H. Sohn, U. Bankwitz, J. Calabrese, Y, Apeloig and T. Müller, *J. Am. Chem. Soc.,* 1995, **117**, 11608–11609.

26 R. West, H. Sohn, D. R. Powell, T. Müller and Y. Apeloig, *Angew. Chem. Int. Ed. Engl.*, 1996, **35**, 1002–1004.

27 B. T. Stępień, T. M. Krygowski and M. K. Cyrański, *J. Org. Chem.*, 2002, **67**, 5987–5992.

28 H. Ottosson, K. Kilså, K. Chajara, M. C. Piqueras, R. Crespo, H. Kato and D. Muthas, *Chem. Eur. J.*, 2007, **13**, 6998–7005.

29 A. P. Scott, I. Agranat, P. U. Biedermann, N. V Riggs and L. Radom, *J. Org. Chem.*, 1997, **62**, 2026–2038.

30 A. Stanger, *J. Org. Chem.*, 2006, **71**, 883–893.

31 For a selection of recent papers on applications of TCNQ and derivatives in organic electronics see e.g.; (a) S. –I. Kato and F. Diederich, *Chem. Commun.* 2010, **46**, 1994–2006; (b) T. –C. Tseng, C. Urban, Y. Wang, R. Otero, S. L. Tait, M. Alcami, D. Écija, M. Trelka, J. M. Gallego, N. Lin, M. Konuma, U. Starke, A. Nefedov, A. Langner, C. Wöll, M. Á. Herranez, F. Martín, N. Martín, K. Kern and R. Miranda, *Nat. Chem.*, 2010, **2**, 374–379; (c) Y. Suzuki, M. Shimawaki, E. Miyazaki, I. Osaka and K. Takimiya, *Chem. Mater.*, 2011*,* **23**, 795–804.

32 A. Kunai, J. Ohshita, T. Iida, K. Kanehara, A. Adachi, and K. Okita, *Synth. Metals*, 2003, **37**, 1007–1008.

33 O. M. Nefedov and M. N. Manakov,. *Angew. Chem. Int. Ed. Engl.*, 1966, **5**, 1021–1038.

34 W. H. Atwell and D. R. Weyenberg, *Angew. Chem. Int. Ed. Engl.*, 1969, **8**, 469–477.

35 P. P. Gaspar and R.West, in *The Chemistry of Organosilicon Compounds*; Wiley; New York, 1998, Vol II, pp 2463–2568.

36 F. Wudl, R. D. Allendoerfer, J. Demirgian and J. M. Robbins, *J. Am. Chem. Soc.*, 1971, **93**, 3160–3162.

37 D. L. Cooper, T. P. Cunningham, J. Gerratt, P. B. Kardakov and M. Raimondi, *J. Am. Chem. Soc.*, 1994, **116**, 4414–4426.

38 D. G. Gilheany, *J. Am. Chem. Soc.*, 1994, **94**, 1339–1374.

39 S. –H. Kang, J. S. Han, M. E. Lee, B. R. Yoo and N. Jung, *Organometallics*, 2003, **22**, 2551–2553.

40 B. Ma, J. –H. Lii, H. F. Schaefer III, and N. L. Allinger, *J. Phys. Chem.*, 1996, **100**, 8763–8769.

41 (a) L. S. Bartell and R. A. Bonham, *J. Chem. Phys.*, 1959, **31**, 400–404; (b) F. H. Allen, O. Kennard, D. G. Watson, L. Brammer, A. G. Orphen and R. Taylor, *J. Chem. Soc., Perkin Trans*., 1987*,* **2**, S1-S19.

42 M. Kaftory, M. Kapon and M. Botoshansky, in *The Chemistry of Organic Silicon Compound*, Vol. 2. Chap 5., p. 181. Wiley, Chichester, UK, Z. Rapport and Y. Apeloig, (Eds).

43 D. M. Mintz and A. Kuppermann, *J. Chem. Phys.*, 1979, **71**, 3499–3513.

44 E. Heilbronner, F. Brogli and E. Vogel, *J. Electron Spectrosc.*, 1976, **9**, 227–239.

45 C. G. Pitt, *J. Am. Chem. Soc.*, 1969, **91**, 6613–6622.

46 A. Wallner, R. Emanuelsson, J. Baumgartner, C. Marschner and H. Ottosson, *Organometallics,* 2013, **32**, 396-405.